FINAL REPORT
to the
Delaware Department of Natural Resources and Environmental Control

Analysis of Speciation Trends Network Data Measured at the State of Delaware

Prepared by

Philip K. Hopke and Eugene Kim

Center for Air Resources Engineering and Science
Clarkson University
Box 5708
Potsdam, NY 13699-5708

January 20, 2005

INTRODUCTION

U.S. EPA established Speciation Trends Networks (STN) to characterize $PM_{2.5}$ (particulate matter ≤ 2.5 μm in aerodynamic diameter) composition in urban areas and to assist identifying areas out of attainment of the promulgated new national ambient air quality standards for airborne particulate matter. Advanced source apportionment studies for the STN $PM_{2.5}$ measurements are needed for developing effective control strategies for $PM_{2.5}$ as well as for the source-specific community epidemiology to relate adverse health effects to apportioned source contributions. Positive matrix factorization (PMF; Paatero, 1997) has been successfully used to assess ambient $PM_{2.5}$ source contributions in the Arctic (Xie et al., 1999), in Hong Kong (Lee et al., 1999), in Thailand (Chueinta et al., 2000), in Phoenix (Ramadan et al., 2000), in Vermont (Polissar et al., 2001), in three northeastern U.S. cities (Song et al., 2001), in a northwestern U.S. city (Kim et al., 2003a), in Seattle (Kim et al., 2004a), and in Atlanta (Kim et al., 2004b).

The objectives of this project are to identify $PM_{2.5}$ sources and estimate their contributions to $PM_{2.5}$ mass concentrations by analysis of the data measured at the EPA STN sites in the State of Delaware. The PMF derived $PM_{2.5}$ sources and their seasonal trends are discussed. The likely locations of the identified sources are suggested using conditional probability function (CPF) and potential source contribution function (PSCF) analyses.

SAMPLE COLLECTION AND CHEMICAL ANALYSIS

The $PM_{2.5}$ samples analyzed in this project were collected on a one-in-six day schedule at the STN monitoring sites located in Wilmington and Dover, Delaware as shown in Figure 1. The monitoring site in Wilmington is located at Martin Luther King Blvd., about 1 km southwest of downtown, 250 m southeast of the bus depot of the Delaware Transit

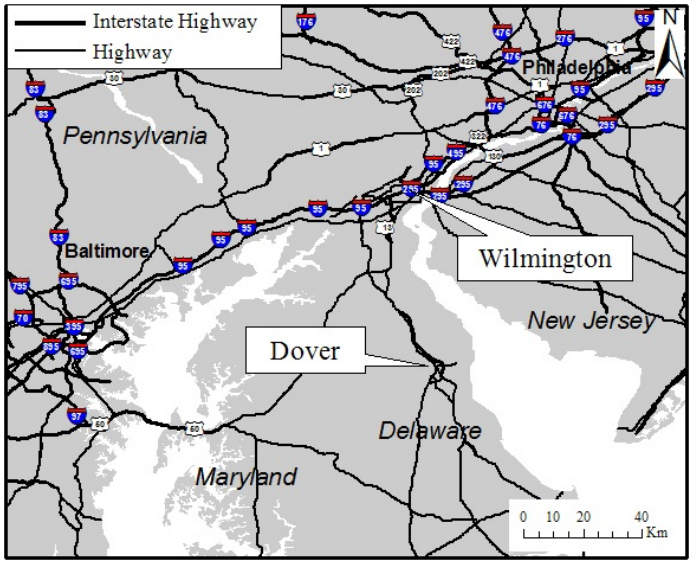

Figure 1. Location of the two STN monitoring sites in Delaware.

Corporation, 3 km northwest of the Port of Wilmington. Interstate highway I-95 and the railroad are closely situated to the west and south of the site, respectively.

The Dover monitoring site is located west of state highways SR1 and Route 13/113. Railroads are situated close to the west of the site. The summary of two monitoring sites are shown in Table 1. Detailed maps of Wilmington and Dover monitoring sites are presented in Figures 2 and 3, respectively. Spiral Aerosol Speciation Samplers (Met One Instruments, Grants Pass, OR) are used at these two sites.

The STN uses multiple analytical laboratories to analyze the samples. There are also differences in the nature of the collected blanks and the treatment of the resulting data. $PM_{2.5}$ samples were collected on Teflon, Nylon, and quartz filters. The Teflon filter was used for mass

Figure 2. Map of Dover, DE showing the location of the STN site.

concentrations and analyzed via any of five different energy dispersive X-ray fluorescence (XRF) spectrometers for the elemental analysis located in three laboratories: Chester LabNet, Cooper Environmental Services, and Research Triangle Institute (RTI). The Nylon filter is analyzed for sulfate (SO_4^{2-}), nitrate (NO_3^-), ammonium (NH_4^+), sodium (Na^+), and potassium (K^+) via ion chromatography (IC). To minimize the sampling artifacts for NO_3^-, a MgO denuder is included at the upstream of the Nylon filter (Koutrakis et al., 1988; Hering et al., 1999). Two instruments for anions and three instruments for cations in RTI were used for the Nylon filter analyses. The quartz filter was analyzed by one of three instruments at RTI via National Institute for Occupational Safety and Health/Thermal Optical Transmittance (NIOSH/TOT) protocol (Birch et al., 1996) for OC and elemental carbon (EC). Carbon denuders that minimize positive sampling artifact caused by adsorption of gaseous organic materials are not included upstream of the quartz filter in the STN samplers (Gundel et al. 1995; Pankow et al., 2001). None of the reported STN data were blank corrected (RTI, 2004a).

Table 1 Summary of STN sites in Delaware.

AIRS code	Monitoring site	Sampler	Latitude	Longitude	sampling period
100032004	Wilmington, DE	SASS [1]	39.7394	-75.5581	June 2001 - Nov. 2003
100010003	Dover, DE	SASS	39.1550	-75.5181	June 2001 - Nov. 2003

[1] Spiral Aerosol Speciation Sampler

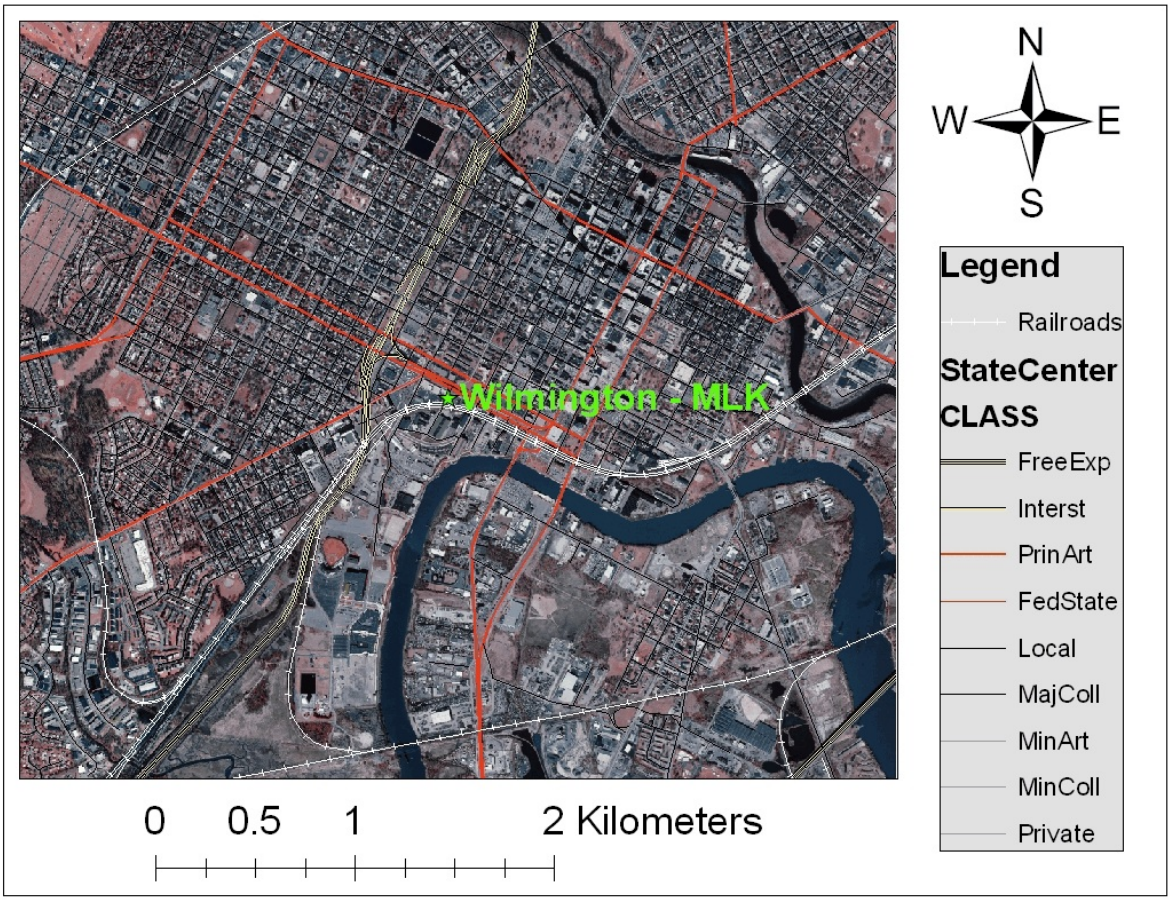

Figure 3. Map of Wilmington, DE showing the location of the STN site.

ESTIMATION OF OC BLANK VALUES

Tolocka et al. (2001) in a comparison study among STN samplers (i.e., Reference Ambient Air Sampler), Federal Reference Method (FRM) sampler, and Versatile Air Pollution Sampler (VAPS) observed that the OC concentration measured by both STN and FRM samplers that did not include carbon denuder at the upstream of quartz filter were consistently higher than the values sampled by VAPS that had a carbon denuder preceding the quartz filter. Since the reported particulate OC concentrations were not blank corrected and there appears to be a positive artifact in the OC concentrations measured by STN samplers, approaches to obtaining an integrated estimate of the OC blank concentrations including trip and field blank as well as OC

positive artifact on quartz filter were tested. One of the ways for this estimation is utilizing the intercept of the regression of OC concentrations against $PM_{2.5}$ (Tolocka et al., 2001).

For the OC blank estimation, samples for which $PM_{2.5}$ or OC mass concentrations were not available were excluded. The sample that showed an extreme OC value on July 7, 2002 caused by a Canadian wildfire was excluded from both data sets from Wilminton and Dover. Comparing co-located $PM_{2.5}$ mass concentrations measured by STN and FRM, outliers (June 24 and November 15, 2001 at Wilmington data set) were censored before the regression analyses between STN $PM_{2.5}$ and OC concentrations.

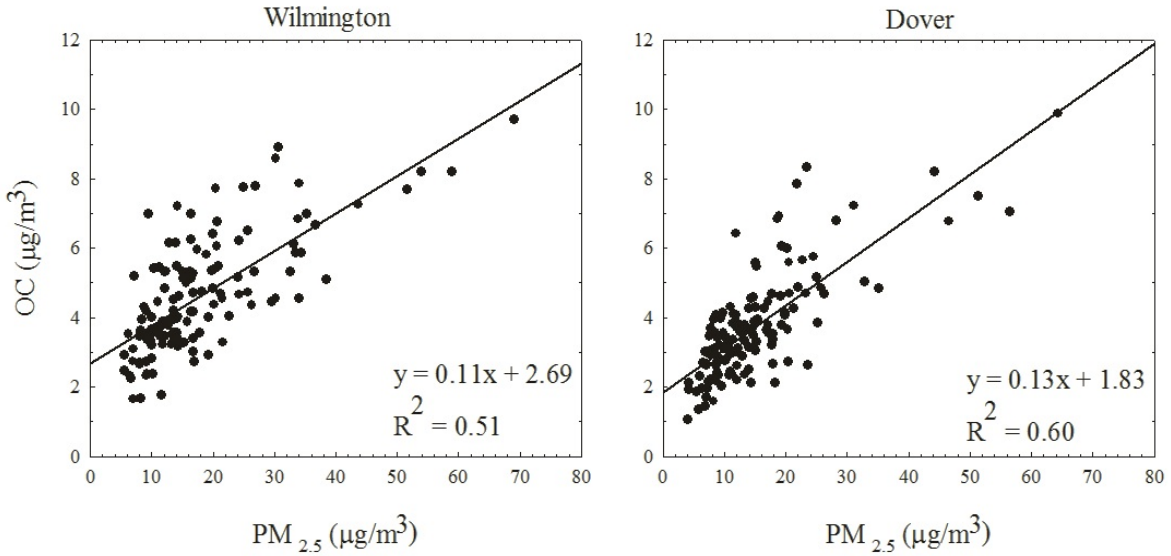

Figure 4. $PM_{2.5}$ versus OC concentration measured at two sites in Delaware.

In Figure 4, $PM_{2.5}$ mass concentrations were compared with OC concentrations for the Wilmington and Dover sites. The intercepts in $PM_{2.5}$ regression against OC concentrations are then considered to be the integrated OC blank concentrations that includes trip blank concentrations as well as positive sampling artifacts by adsorption of gaseous organic matter. The results for the two monitoring sites are summarized in Table 2. For the source apportionment study, the reported STN OC concentrations were blank corrected by subtracting the estimated OC blank concentrations from the measured values.

Table 2. Summary of OC blank concentrations estimated from regression of $PM_{2.5}$ mass concentrations against OC concentrations.

Monitoring site	OC blank ($\mu g/m^3$)
Wilmington, DE	2.69
Dover, DE	1.83

METHOD DETECTION LIMIT VALUES AND ERROR ESTIMATES

The application of PMF depends on the estimated uncertainties for each of the measured data. The uncertainty estimation based on the analytical uncertainties and laboratory method detection limit (MDL) values provides a useful tool to decrease the weight of missing and below detection limit (BDL) data in these methods. Polissar et al. (1998) suggested a procedure for estimating uncertainties for the PMF study of seven Interagency Monitoring of Protected Visual Environments (IMPROVE) $PM_{2.5}$ speciation data sets, in which data uncertainties and MDL values were well defined. In STN data, various instruments were used to analyze samples and they produce different MDL values and analytical uncertainties. Since prior to July 2003, the STN data were not accompanied by MDL values and uncertainties, it is not possible to identify which instrument was used for the analysis of any particular sample and thus, it is not possible to assign its particular MDL values and uncertainties for that sample. Therefore, a comprehensive set of MDL values and error structures that can be used for source apportionment studies are estimated as described by Kim et al. (2005a).

From the investigation of appropriate MDL values for PMF analyses, the average MDL values among MDL values from five XRF spectrometers (Chester770, Chester771, Cooper, RTI1, RTI2) were selected for this project and presented in Table 3.

A limited set of the XRF analytical uncertainties for thirteen eastern STN sites for samples collected between March 2001 and November 2003 were acquired from the U.S. EPA. The reported analytical uncertainties for S, Si, K, and Fe from the five instruments in three laboratories were compared in Figure 5. Various species, instruments, and laboratories show different analytical uncertainty structures. As can be seen from the Figure 5, the uncertainties are given as

fractions of measured mass concentrations. To develop a comprehensive set of errors that could be used for PMF studies across the STN, a general fractional error was estimated by comparing the available measured concentrations and their associated uncertainties. To generate the error structures, the fractional errors that are estimated as a fraction of the measured concentrations are chosen to encompass most of the reported uncertainties as shown by the lines in Figure 5 and to provide the most reasonable PMF solution. The specific values for each element are shown in Table 3. Thus, based on the studies of Polissar et al. (1998), the error structures (s_{ij}) were calculated using the following equation:

$$s_{ij} = \left[MDL_j\right]/3 + k \cdot x_{ij} \quad (1)$$

where x_{ij} is the jth species concentration measured in the ith sample and the values of k are given in Table 3.

Table 3. Estimated MDL values and fractional uncertainties for the EPA STN data measured at Wilmington and Dover, DE.

Species	Method detection limit (ng/m^3)	Uncertainty (%)
PM_{25}	746.27	7.0
OC	243.78	7.0
EC	243.78	7.0
SO_4^{2-}	12.44	7.0
NH_4^+	16.58	7.0
NO_3^-	8.71	7.0
K^+	13.89	7.0
Na^+	30.06	7.0
Al	16.43	10.0
Sb	22.16	5.0
As	7.07	20.0
Ba	34.65	5.0
Br	1.81	5.0
Cd	10.45	5.0
Ca	5.18	11.0
Ce	52.55	5.0
Cs	24.55	5.0
Cl	8.33	10.0
Cr	1.81	5.0

Co	1.47	10.0
Cu	1.92	5.0
Eu	6.95	5.0
Ga	3.73	5.0
Au	5.90	5.0
Hf	22.03	5.0
In	12.90	5.0
Ir	7.28	5.0
Fe	2.00	5.0
La	41.08	5.0
Pb	4.72	5.0
Mg	23.23	5.0
Mn	2.04	5.0
Hg	4.22	5.0
Mo	6.98	5.0
Ni	1.45	5.0
Nb	4.30	5.0
P	7.58	10.0
K	7.07	10.0
Rb	2.03	5.0
Sm	5.38	5.0
Sc	1.55	5.0
Se	2.46	5.0
Si	12.48	10.0
Ag	9.36	5.0
Na	78.54	10.0
Sr	2.40	5.0
S	10.02	11.0
Ta	14.53	5.0
Tb	5.81	5.0
Sn	18.38	5.0
Ti	3.52	5.0
V	2.34	5.0
W	11.24	5.0
Y	2.93	5.0
Zn	1.98	5.0
Zr	3.60	5.0

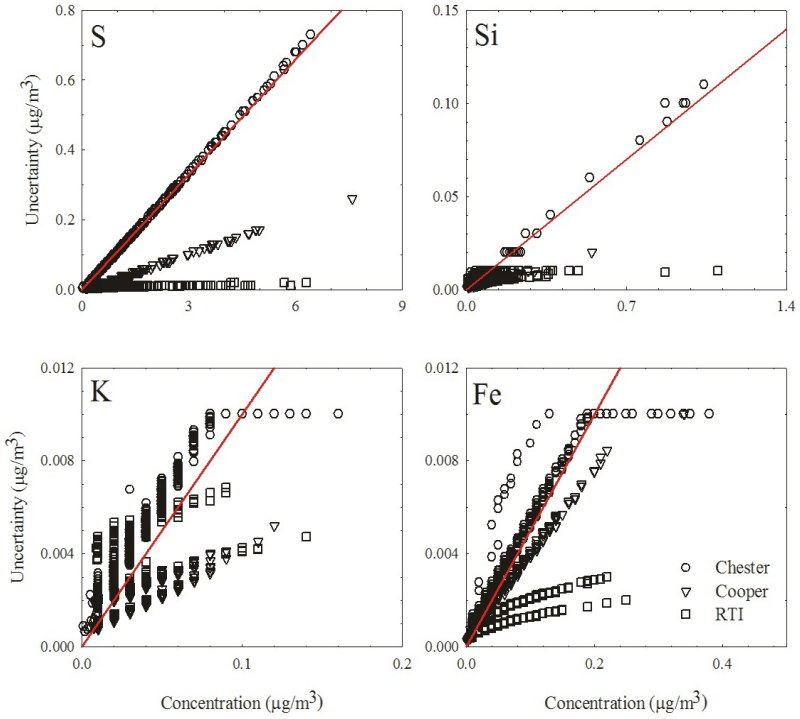

Figure 5. The comparison between measured concentrations and associated uncertainties.

MULTIVARIATE RECEPTOR MODELING

An ambient $PM_{2.5}$ compositional data set of 24-hour integrated samples collected at a STN site in Burlington, VT were analyzed through the application of PMF to examine the estimated error structures and to investigate the appropriate MDL values. The receptor modeling problem can be expressed in terms of the contribution from p independent sources to all chemical species in a given sample as follows (Miller et al., 1972; Hopke, 1985),

$$x_{ij} = \sum_{s=1}^{p} g_{is} f_{sj} + e_{ij} \tag{2}$$

where g_{is} is the particulate mass concentration from the sth source contributing to the ith sample, f_{sj} is the jth species mass fraction from the sth source, e_{ij} is residual associated with the jth species concentration measured in the ith sample, and p is the total number of independent sources. PMF

provides a solution that minimizes an object function, *Q(E)*, based upon uncertainties for each observation (Polissar et al., 1998; Paatero, 1997).

$$Q(E) = \sum_{i=1}^{n} \sum_{j=1}^{m} \left[\frac{x_{ij} - \sum_{s=1}^{p} g_{is} f_{sj}}{u_{ij}} \right]^2 \quad (3)$$

where u_{ij} is an uncertainty estimate in the *j*th constituent measured in the *i*th sample.

There are an infinite number of possible combinations of source contribution and profile matrices to the multivariate receptor modeling problem due to the free rotation of matrices (Henry, 1987). PMF uses non-negativity constraints on the factors to decrease rotational ambiguity. Also, the parameter FPEAK and the matrix FKEY are used to control the rotations (Lee et al., 1999; Paatero et al., 2002). By setting a non-zero values of FPEAK, the routine is forced to add one source contribution vector to another and subtract the corresponding source profile factors from each other and thereby yield more physically realistic solutions. PMF was run with different FPEAK values to determine the range within which the scaled residuals remains relatively constant (Paatero et al., 2002; Kim et al., 2003b). The optimal solution should lie in this FPEAK range. In this way, subjective bias was reduced to a large extent. External information can be imposed on the solution to control the rotation. If specific species in the source profiles are known to be zero, then it is possible to pull down those values towards lower concentration through appropriate settings of FKEY resulting in the most interpretable source profiles. Each element of the FKEY matrix controls the pulling-down of the corresponding element in the source profile matrix by setting a non-zero integer values in FKEY matrix (Lee et al., 1999).

Based on the studies of Polissar et al. (1998), the measured concentrations below the MDL values were replaced by half of the MDL values and their uncertainties were set at 5/6 of the MDL values. Missing concentrations were replaced by the geometric mean of the concentrations and their accompanying uncertainties were set at four times of this geometric mean concentration.

For the application of PMF, only samples for which $PM_{2.5}$ or OC mass concentrations were not available were excluded from data set measured at Wilmington and Dover sites. To obtain reasonable model fit, the Canadian wildfire sample on July 7, 2002 in which $PM_{2.5}$ and OC mass concentrations were unusually high was excluded in the source apportionment study. Overall, 21 and 18 % of the original data was excluded from Wilmington and Dover data, respectively. XRF S and IC SO_4^{2-} showed excellent correlations (*slope* = 3.4, r^2 = 0.98 for Wilmington data; *slope* = 3.2, r^2 = 0.96 for Dover data), so it is reasonable to exclude XRF S from the analysis to prevent double counting of mass concentrations. Also, IC Na^+ and IC K^+ were chosen due to the higher analytical precision compared to XRF Na and XRF K. Chemical species that have values more than 90 % below MDL were excluded. Thus, a total of 117 samples and 29 species including $PM_{2.5}$ mass concentrations and a total of 122 samples and 30 species including $PM_{2.5}$ mass concentrations collected between June 2001 and November 2003 were used for the Wilmington and Dover analyses, respectively.

Species that have Signal/Noise (S/N) ratios between 0.2 and 2 were considered weak variables and their estimated uncertainties were increased by a factor of five to reduce their weight in the solution as recommended by Paatero and Hopke (2003). The Nylon filters were contaminated with Na^+ between October 2001 and January 2002 and were reported with error flags (RTI, 2004b). Their estimated uncertainties were increased by a factor of thirty. Summaries of $PM_{2.5}$ speciation data and S/N ratios are provided in Tables 4 and 5.

In these analyses, the measured $PM_{2.5}$ mass concentration was included as an independent variable in the PMF modeling to directly obtain the mass apportionment without the usual multiple regression. The utilization of $PM_{2.5}$ mass concentration as a variable is specified in detail in Kim et al. (2003b)

Finally, to obtain physically reasonable PMF solution, it was necessary to test different numbers of sources and different FPEAK values with the final choice based on the evaluation of the resulting source profiles as well as the quality of the species fits. The global optimum of the PMF solutions were tested by using multiple random starts for the initial values used in the iterative fitting process.

CONDITIONAL PROBABILITY FUNCTION ANALYSIS

The conditional probability function (CPF) (Kim et al., 2003b) was calculated to analyze point source impacts from various wind directions using source contribution estimates from PMF coupled with wind direction values measured on site. The same daily fractional contribution was assigned to each hour of a given day to match to the hourly wind data. The CPF is defined as

$$CPF = \frac{m_{\Delta\theta}}{n_{\Delta\theta}} \quad (4)$$

where $m_{\Delta\theta}$ is the number of occurrence from wind sector $\Delta\theta$ that exceeded the threshold criterion, and $n_{\Delta\theta}$ is the total number of data from the same wind sector. In this study, 16 sectors were used ($\Delta\theta$ = 22.5 degrees). Calm winds (< 1 m/sec) were excluded from this analysis due to the isotropic behavior of wind vane under calm winds. From tests with several different percentile of the fractional contribution from each source, the threshold criterion of the upper 25 percentile was chosen to clearly show the directionality of the sources. The sources are likely to be located to the direction that have high conditional probability values.

POTENTIAL SOURCE CONTRIBUTION FUNCTION

To identify the likely locations of the regional sources for the secondary sulfate aerosols, the potential source contribution function (PSCF) (Ashbaugh et al., 1985; Hopke et al., 1995) was calculated using the source contributions estimated from PMF and backward trajectories calculated using the Hybrid Single Particle Lagrangian Integrated Trajectory (HYSPLIT) model (Draxler et al., 2003; Rolph et al., 2003). Five-day backward trajectories starting at height of 500 m above the actual ground level were computed using the vertical mixing model every day producing 120 trajectories per sample. The geophysical region covered by the trajectories was divided into grid cells of 1° × 1° latitude and longitude so that there are an average of 2 trajectory end points per cell. If a trajectory end point of the air parcel lies in the *ij*th cell, the trajectory is assumed to collect $PM_{2.5}$ emitted in the cell. Once the $PM_{2.5}$ is incorporated into the air parcel, it is assumed to be transported along the trajectory to the monitoring site. $PSCF_{ij}$ is the conditional probability that an air parcel that passed through the *ij*th cell had a high concentration upon arrival at the monitoring site defined as

$$PSCF_{ij} = \frac{m_{ij}}{n_{ij}} \tag{5}$$

where n_{ij} is the total number of end points that fall in the ijth cell and m_{ij} is the number of end points in the same cell that are associated with samples that exceeded the threshold criterion. In this study, the average contribution of each source was used for the threshold criterion. The sources are likely to be located in the area that have high PSCF values.

To minimize the effect of small values of n_{ij} that result in high PSCF values with a high uncertainties, an arbitrary weight function $W(n_{ij})$ was applied to downweight the PSCF values for the cell in which the total number of end points was less than three times the average number of the end points per cell (Hopke et al., 1995; Polissar et al., 2001).

$$W(n_{ij}) = \begin{cases} 1.0 & 8 < n_{ij} \\ 0.7 & 3 < n_{ij} \leq 8 \\ 0.4 & 2 < n_{ij} \leq 3 \\ 0.2 & 2 \leq n_{ij} \end{cases} \tag{6}$$

Table 4. Summary of $PM_{2.5}$ species mass concentrations at Wilmington, DE.

Species	Arithmetic mean (ng/m^3)	Geometric mean (ng/m^3)	Minimum (ng/m^3)	Maximum (ng/m^3)	Number of below MDL values (%)	Number of missing values (%)	S/N ratio
$PM_{2.5}$	18539.3	16432.4	5500.0	69100.0	0	0	28.5
OC	2171.4	1540.2	20.0	10310.0	5.1	0	11.3
EC	821.5	752.5	255.0	2260.0	0	0	3.7
S	1819.4	1438.6	312.0	9490.0	0	0	222.6
NH_4^+	2544.0	2003.1	179.0	11400.0	0	0	189.6
NO_3^-	2575.0	1884.3	261.0	10100.0	0	0	379.5
Al	22.8	15.5	1.3	245.0	73.5	0	1.8
Ba	36.6	32.0	0.7	98.1	65.8	0	1.0
Br	3.9	3.2	0.1	12.7	20.5	0	2.3
Ca	35.5	31.4	6.5	90.3	0.0	0	7.4
Cl	35.1	14.3	0.1	344.0	62.4	0	6.6
Cr	1.8	1.4	0.1	5.3	63.2	0	1.0
Cu	13.2	8.9	0.1	95.3	2.6	0	9.8
Fe	112.3	95.0	26.0	437.0	0.0	0	63.6
Pb	5.6	4.3	0.2	41.6	63.2	0	1.3
Mg	26.9	20.5	0.1	213.0	88.9	0	1.0
Mn	3.5	2.7	0.2	15.2	42.7	0	1.9
Ni	4.2	3.3	0.6	13.6	12.8	0	3.2
P	6.6	6.0	0.1	17.9	88.9	0	0.5
K	74.8	64.9	17.1	268.0	70.1	0	3.4
Se	2.1	1.8	0.1	6.5	70.9	0	0.9
Si	78.2	63.6	5.6	496.0	0.9	0	7.9
Na	225.7	141.9	1.0	1610.0	6.0	0.4	11.6
Sr	1.7	1.6	0.1	18.5	88.9	0	0.8
Ta	14.5	12.1	0.9	45.4	76.9	0	0.9
Sn	11.9	11.7	1.4	42.8	82.9	0	0.6
Ti	6.4	4.9	0.2	21.5	29.9	0	2.1
V	7.8	5.9	0.6	27.3	12.8	0	4.0
Zn	12.8	9.0	0.5	98.8	4.3	0	8.8

Table 5. Summary of $PM_{2.5}$ species mass concentrations at Dover, DE.

Species	Arithmetic mean (ng/m^3)	Geometric mean (ng/m^3)	Minimum (ng/m^3)	Maximum (ng/m^3)	Number of below MDL values (%)	Number of missing values (%)	S/N ratio
$PM_{2.5}$	15235.2	13344.8	4200.0	64300.0	0	0	24.0
OC	1983.5	1396.3	15.0	8045.0	4.9	0	10.4
EC	467.8	406.9	12.9	1320.0	10.7	0	2.1
S	1599.3	1248.8	359.0	8860.0	0	0	201.1
NH_4^+	1960.9	1445.3	48.1	11800.0	0	0	153.9
NO_3^-	1812.2	1306.5	245.0	8480.0	0	0	279.9
Al	19.6	14.4	0.5	152.0	78.7	0	1.2
Ba	34.9	29.4	0.4	95.8	62.3	0	1.0
Br	3.2	2.6	0.1	8.2	27.9	0	1.8
Ca	33.7	24.4	4.8	240.0	3.3	0	8.7
Ce	28.1	28.5	0.2	99.2	87.7	0	0.5
Cl	23.7	10.6	0.2	348.0	74.6	0	4.6
Cr	1.5	1.2	0.1	9.1	82.8	0	0.9
Cu	3.1	2.0	0.1	12.1	61.5	0	2.0
La	20.6	23.5	0.2	75.8	88.5	0	0.5
Pb	3.5	3.0	0.0	12.3	78.7	0	0.7
Mn	2.0	1.7	0.1	6.7	62.3	0	1.0
Ni	2.2	1.6	0.1	7.9	45.1	0	1.7
K	64.2	57.4	3.1	115.0	70.5	0	2.7
Sc	0.9	0.8	0.1	3.2	86.9	0	0.4
Se	1.9	1.7	0.0	8.6	75.4	0	0.8
Si	82.3	59.7	3.3	554.0	1.6	0	9.2
Na	262.0	161.3	4.2	1650.0	6.6	0	12.8
Sr	1.7	1.5	0.1	9.7	87.7	0	0.7
Ta	12.0	10.4	0.5	50.8	81.1	0	0.8
Sn	12.3	12.0	0.1	56.0	81.1	0	0.7
Ti	4.9	3.7	0.3	25.2	47.5	0	1.7
V	3.3	2.6	0.1	11.2	43.4	0	1.6
Zn	6.8	4.6	0.1	44.9	22.1	0	4.5

RESULTS AND DISCUSSION

A variety of factor number solutions were explored for Wilmington and Dover data sets. A nine-source model and a value of FPEAK = 0 provided the most physically reasonable source profiles for the Wilmington data. For the Dover data, six-source model, a value of FPEAK = 0, and a FKEY matrix provided the most reasonable source profiles. For the FKEY matrix, values of all elements were set to zero, except: value of 5 for NH_4^+ in airborne soil. The average source contributions of each source to the $PM_{2.5}$ mass concentrations are provided in Tables 6 and 7.

Table 6. Average source contributions to $PM_{2.5}$ mas concentration at Wilmington, DE.

Sources	Average source contribution (standard error)	
	Mass concentration ($\mu g/m^3$)	Percentile (%)
Secondary sulfate	6.97 (0.72)	37.9 (3.9)
Secondary nitrate	3.12 (0.28)	17.0 (1.5)
Gasoline vehicle	2.18 (0.17)	11.9 (0.9)
Oil combustion	1.52 (0.11)	8.3 (0.6)
Railroad	1.10 (0.08)	6.0 (0.4)
Airborne soil	1.09 (0.11)	6.0 (0.5)
Aged sea salt	1.03 (0.11)	5.6 (0.6)
Bus depot	0.79 (0.09)	4.3 (0.5)
Diesel emissions	0.57 (0.06)	3.1 (0.3)

Table 7. Average source contributions to $PM_{2.5}$ mas concentration at Dover, DE.

Sources	Average source contribution (standard error)	
	Mass concentration ($\mu g/m^3$)	Percentile (%)
Secondary sulfate	7.50 (1.45)	49.6 (9.6)
Gasoline vehicle	2.38 (0.35)	15.8 (2.3)
Secondary nitrate	1.50 (0.30)	9.9 (2.0)
Aged sea salt	1.44 (0.27)	9.5 (1.8)
Diesel emissions	1.19 (0.20)	7.9 (1.3)
Airborne soil	1.11 (0.21)	7.3 (1.4)

In Figure 6, comparisons of the daily reconstructed $PM_{2.5}$ mass contributions from all sources with measured $PM_{2.5}$ mass concentrations shows that the resolved sources effectively reproduce the measured values and account for most of the variation in the $PM_{2.5}$ mass concentrations (*slope* = 0.95 ± 0.02 and r^2 = 0.95 for Wilmington; *slope* = 1.04 ± 0.02 and r^2 = 0.94 for Dover). In Figure 7, the averaged seasonal contributions from each source are compared (summer: April - September; winter: October - March). The source profiles, corresponding source contributions, CPF plots, and weekday/weekend variations are presented in Figures 8 - 15.

Secondary sulfate aerosols are represented by its high concentrations of SO_4^{-2} and NH_4^+. Secondary sulfate had the highest source contribution to $PM_{2.5}$ mass concentrations accounting for 38 % (7.0 $\mu g/m^3$) and 50 % (7.5 $\mu g/m^3$) of the $PM_{2.5}$ mass concentration at Wilmington and Dover, respectively. As shown in Figures 7, 9 and 13, the secondary sulfate factor show strong seasonal variation with higher concentrations in summer when the photochemical activity is highest indicating origination from coal-fired electricity generating plants. When compared to the studies based on Interagency Monitoring of Protected Visual Environments (IMPROVE) data in which PMF separated summer and winter-high secondary sulfate aerosols with seasonal

differences of the Se/S concentrations (Kim and Hopke, 2004a, b; Kim et al., 2005b), the Se data were inadequate to permit the winter-high secondary sulfate aerosol to be extracted in this analyses.

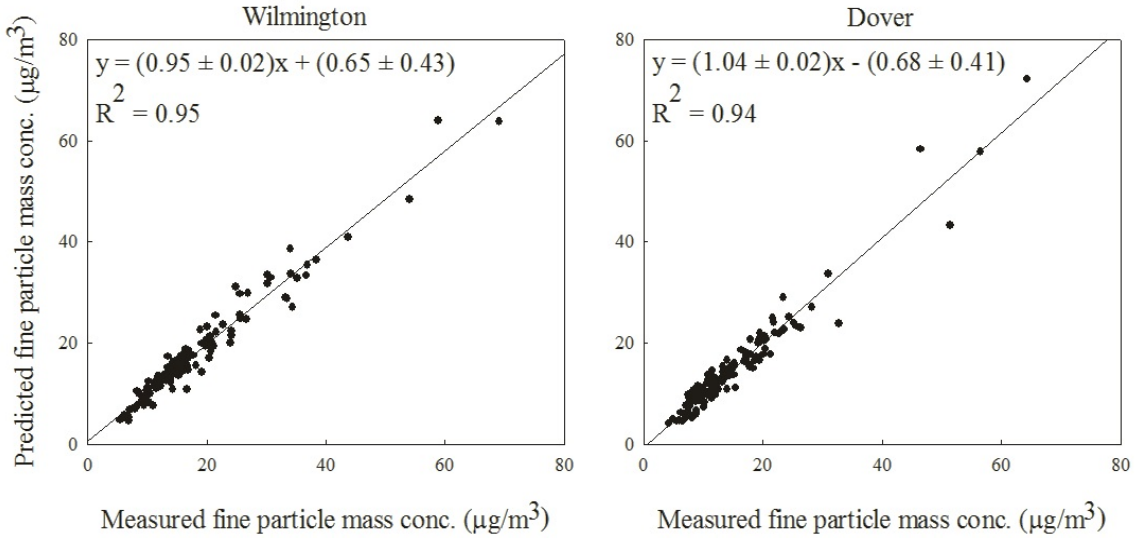

Figure 6. Measured versus PMF predicted $PM_{2.5}$ mass concentrations

In Figures 9 and 13, both monitoring sites were impacted by high concentrations of secondary sulfates aerosols: 48.5 µg/m^3 (Wilmington) and 43.9 µg/m^3 (Dover) on July 19, 2002; 45.8 µg/m^3 (Wilmington) and 51.7 µg/m^3 (Dover) on June 26, 2003. The air mass backward trajectories were calculated for the days with high impacts using the HYSPLIT model starting height of 500 m above sea level using the vertical mixing model. As shown in Figures 16 and 17, the elevated contributions in both Wilmington and Dover were likely to be caused by the regional transport of secondary aerosols from midwestern coal-fired power plants in the Ohio River Valley (Poirot et al., 2001).

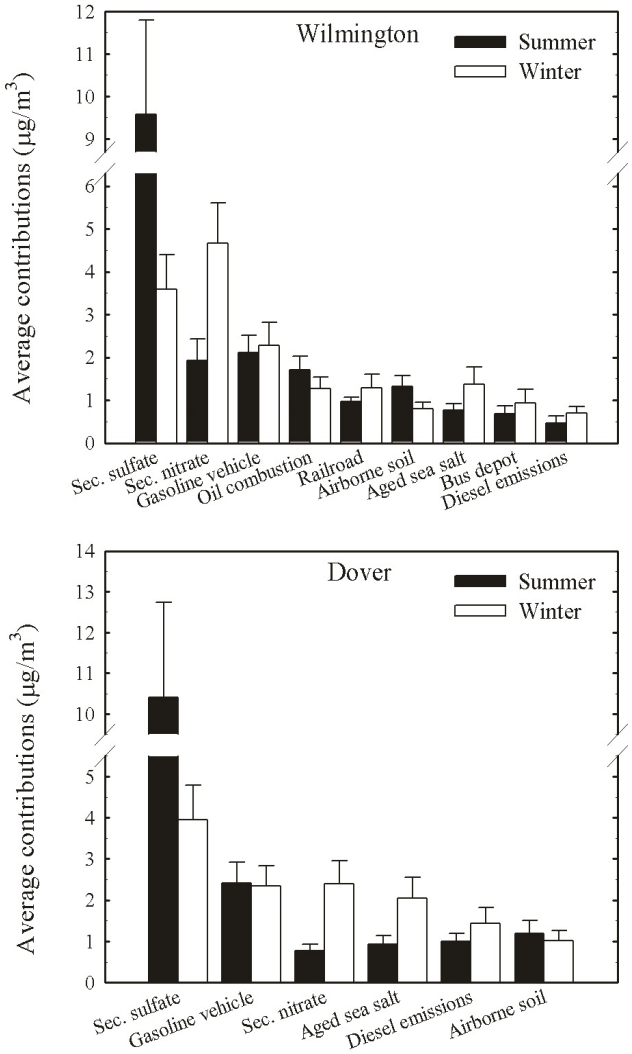

Figure 7. The seasonal comparison of source contributions to $PM_{2.5}$ mass concentration (mean ± 95 % confidential interval)

The PSCF plots for the secondary sulfate aerosol are shown in Figure 18 in which PSCF values are displayed in terms of a color scale. Potential source areas and pathways that give rise to the high contribution to the Wilmington site are located in Mississippi, northern Alabama, Georgia, Tennessee, western South Carolina, and southern Kentucky. These identified areas also include areas where the secondary sulfate aerosols were formed in addition to areas where the sources were located. There remain some potential source areas in the Ohio River Valley as well as St. Louis, MO. The PSCF plot for Dover sites shows high values around southeastern Kentucky, northern Alabama, and the coast of the southern Mississippi, Alabama, and Florida. There are significant petrochemical industries along the coast, but the detailed nature of these source areas is uncertain. There are also areas of potential influence in Georgia.

The prior PSCF analysis for IMPROVE data measured at Washington, DC (Kim and Hopke, 2005c) showed that the high potential areas of the summer and winter-high secondary sulfate aerosols included Ohio River Valley, southern Kentucky, Tennessee, southern Louisiana, Mississippi, and Alabama. The potential source areas of secondary sulfate aerosols contributing Delaware and Washington, DC are very similar, and it confirms our source apportionment studies with STN data.

Secondary nitrate aerosol is represented by its high concentration of NO_3^- and NH_4^+. The average contributions of this source to the $PM_{2.5}$ mass concentrations were 3.1 $\mu g/m^3$ and 1.5 $\mu g/m^3$ at Wilmington and Dover, respectively. This source has seasonal variation with maxima in winter as shown in Figures 7, 9, and 13. These peaks in winter indicate that low temperature and high relative humidity help the formation of nitrate aerosols. Particulate nitrate requires both the formation of HNO_3 from NO_x and the availability of NH_3 from a variety of emissions including animal husbandry, people, and spark-ignition vehicles. Although the CPF plots for both sites show the contributions from Philadelphia, PA and Baltimore, MD, it is likely that the ammonium nitrate arises from a combination of local and regional emissions.

Gasoline vehicle and diesel emissions are represented by high OC and EC, whose abundances differ between these sources (Watson et al., 1994). Gasoline vehicles emissions have high concentration of the OC. In contrast, diesel emissions were tentatively identified on the basis of the high concentration of EC. The CPF plots of gasoline vehicle and diesel emissions at the Wilmington site largely follow a line connecting 60° and 240°. Interstate highway I-95 runs from the southwest to the northeast of the site roughly in the direction indicated by the CPF plots. In addition, the plots indicate some impact from the downtown area located northeast of the site. Gasoline vehicle emissions do not show a strong weekday/weekend variations. In contrast, diesel emissions show weekday-high variations demonstrating that diesel emissions are from heavy-duty vehicles operating more on weekdays.

Another factor with high concentration of OC and EC was identified in Wilmington. It has a high concentration of Cu that might come from the metallic brakes used on large vehicles and has commonly been seen in diesel profiles in other studies (Kim and Hopke, 2004a,b; Kim et al., 2004a,b). The site in Wilmington is near to a bus depot as shown in Figure 2. This source may represent the emissions from the bus depot. The CPF plots of this source indicate impacts from bus depot located west of the site. The bus depot profile does not include Zn and Ca that are often seen in the diesel emissions profiles. These elements appear in the separate diesel emissions profile and may be more strongly related to the on-road trucks moving at higher speed. The bus depot does not show strong weekday/weekend variations as shown in Figure 11.

A third high-EC source was identified in Wilmington that has been tentatively assigned to

be a combination of emissions from the nearby railroad and the Port of Wilmington. The main line AMTRAK tracks run parallel to the river to the south of the site, and the passenger terminal is situated southeast of the site. Although a large fraction of the trains are electric powered, there are a number of commuter and AMTRAK trains that use diesel engines. The profile contains a significant Fe concentration that was reported to be the major species emitted by electric trains in Zurich, Switzerland (Bukowiecki et al., 2004). The CPF plot of this source shows the contributions from southwest and southeast where the railroads and the Port of Wilmington are located. Railroad emission shows weekday-high variations. It appears that there may be directional specificity to help resolve multiple point sources of carbonaceous aerosol in Wilmington.

In Figure 14, the CPF plots for gasoline and diesel emissions identified in Dover indicate impacts from the highway junctions located northeast and southeast of the site, and the residential area located south and southwest of the site. The high diesel impact from west and high S concentration in source profile indicate that diesel emissions identified in Dover site are likely to be a combination of emissions from the nearby railroad and on-road diesel vehicles. Gasoline vehicle and diesel emissions do not show strong weekday/weekend variations in the Dover site.

The average $PM_{2.5}$ mass contributions from gasoline vehicle, diesel emissions, bus depot, and railroad were 2.2, 0.6, 0.8, and 1.1 $\mu g/m^3$ in Wilmington, respectively. In Dover, gasoline vehicle and diesel emissions contributed 2.4 and 1.2 $\mu g/m^3$ to $PM_{2.5}$ concentration.

Oil combustion is characterized by carbon fractions, V, and Ni. This source contributes 1.5 $\mu g/m^3$ to the $PM_{2.5}$ mass concentration in Wilmington. As shown in Figure 8, this source profile has large amount of EC reflecting residual oil combustion. This source does not show strong weekday/weekend variations. The CPF plot of this source in Figure 10 points to the northeast and southeast. Previous backward trajectory analyses for the Vermont aerosol study indicated that major sources of oil combustion were located along northeastern urban corridor between Washington, DC and Boston, MA (Polissar et al., 2001). There is a refinery in Delaware City which is south of the site and a large oil-fired power plant within a few km of this site to the south-south east. This plant also burns a significant quantity of coal in addition to residual oil. From the CPF plot, it appears that the Wilmington site is sufficiently close to oil-fired power plant

that the plume rarely affects this site. There is a large oil-fired power plant in Salisbury, MD (soutwest) and another moderate sized plant in Dover, DE (south). These sources may contribute to the southerly probabilities. It is also possible that part of these source contributions is actually ship emissions from the direction of the Port of Wilmington. This source shows summer-high seasonal variation that tends to favor an assignment of oil fired power plants.

The airborne soil is represented by Si, Al, and Ca (Watson et al., 2001a, 2001b) contributing 1.1 $\mu g/m^3$ to the $PM_{2.5}$ mass concentration at both Wilmington and Dover sites. Crustal particles could be contributed by roads, construction sites, and wind-blown soil dust. There is a low background of contributions of soil throughout the year that are due to such local sources. There are seasonal variations with higher concentrations in the dry summer season. Prior STN data analysis for Burlington, VT (Kim et al., 2005a) identified the influence of a Saharan dust storm event on July 4, 2002. However, since the samples were not collected between July 1 and 7, 2002, this dust storm event was not identified in this analysis. The elevated contribution of airborne soil on July 19, 2002 and June 26, 2003 at Wilmington shown in Figure 9 were likely related to the regional transport from Midwest noted earlier (also shown in Figures 16 and 17), but could also represent small contributions from intercontinental dust transport. Figure 19 shows the air mass backward trajectories for 20 days, and the likely locations suggest that the elevated contribution on September 11, 2002 at Dover (in Figure 13) was not likely caused by a regional dust storm. There is only a small increase in the soil contribution in Wilmington such that it seems likely that this single high value is the result of a local event.

Aged sea salt is characterized by its high concentration of Na, SO_4^{2-} and NO_3^-. The lack of chlorine in the profile is presumed to be caused by chloride displacement by acidic gases. It also suggests that the particles are aged sea salt and not local road salt. Road salt would be expected to retain its chlorine and would be only seen during the winter months. Aged sea salt accounts for 1.0 and 1.4 $\mu g/m^3$ of the $PM_{2.5}$ mass concentrations in Wilmington and Dover, respectively. This source shows a winter-high seasonal pattern. Although the contaminated Na^+ collected between October 2001 and January 2002 were down-weighted in PMF analyses, the source contributions of aged sea salt in this period were relatively high. Therefore, there is a possibility that this source contribution is still inflated to some degree by this contamination.

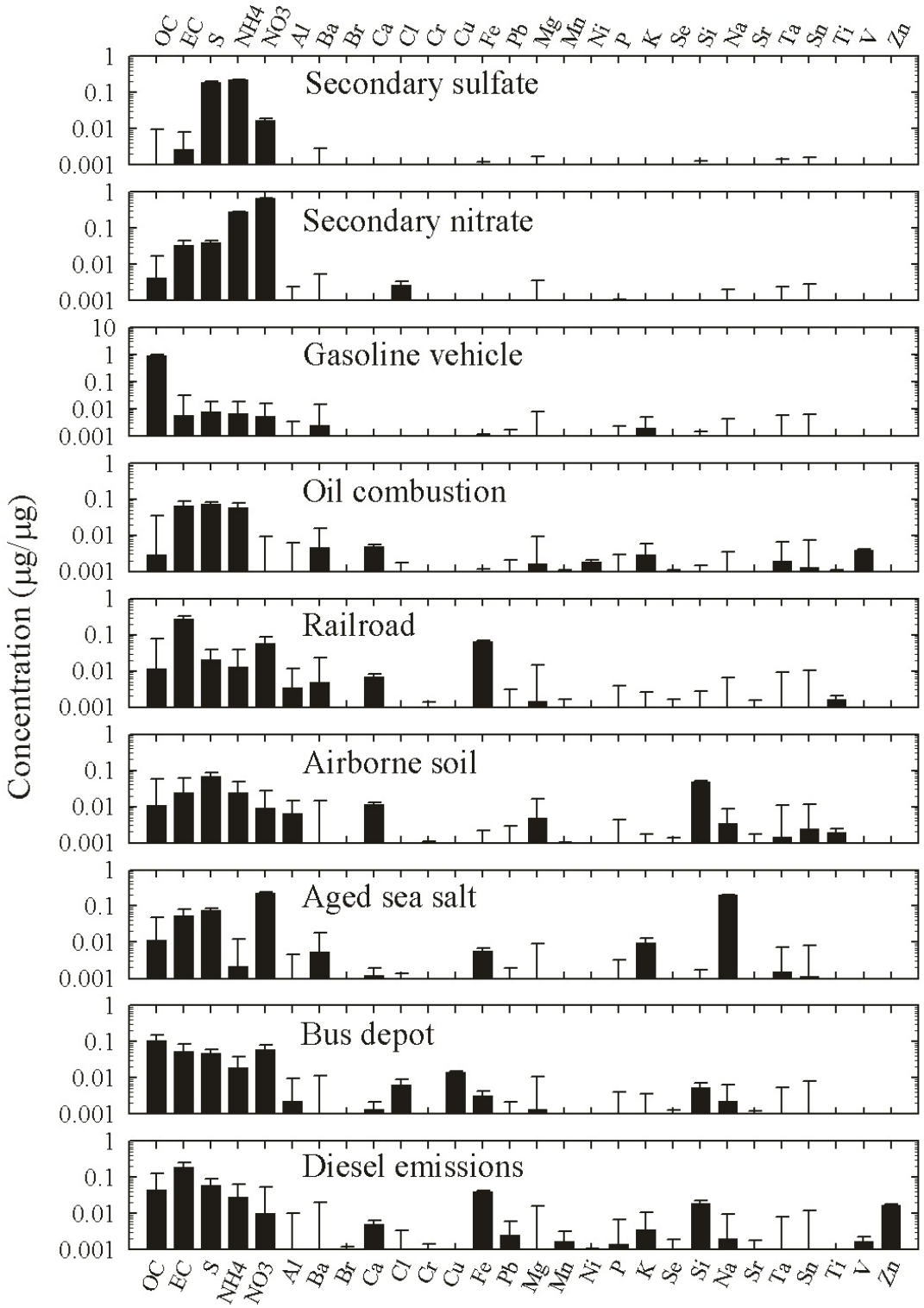

Figure 8. Source profiles deduced from $PM_{2.5}$ samples measured at Wilmington site (prediction ±standard deviation).

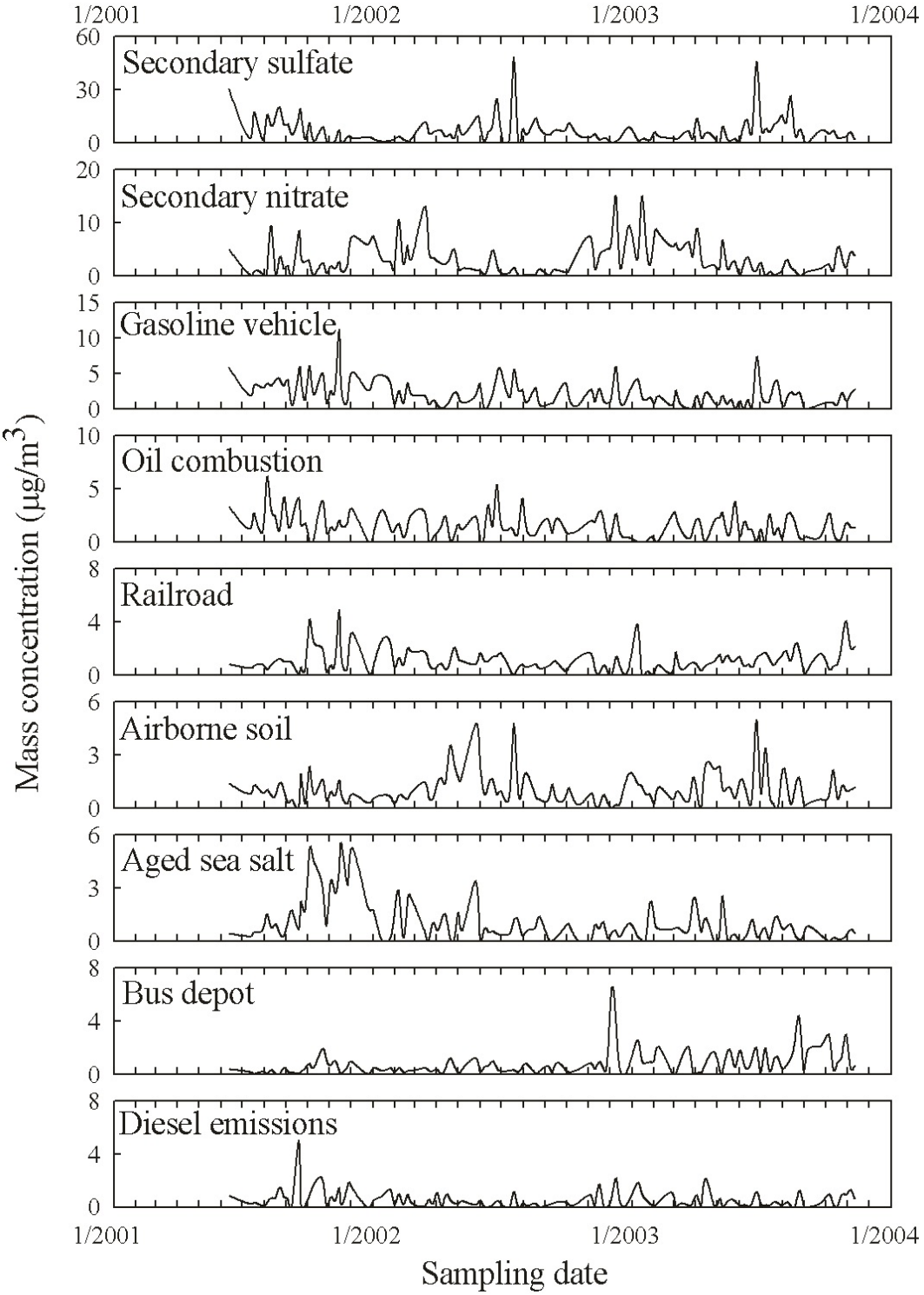

Figure 9. Time series plots of source contributions at Wilmington site.

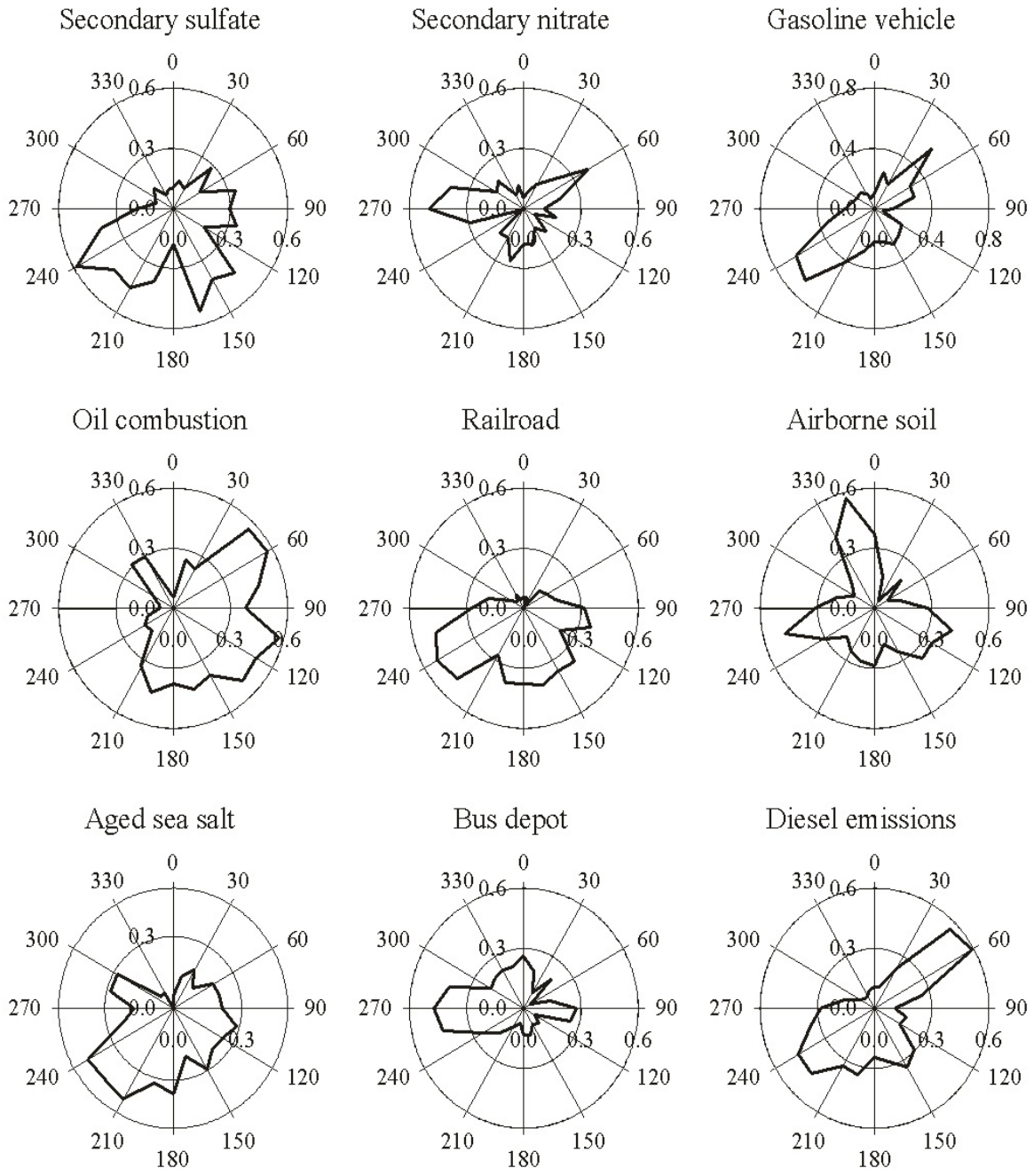

Figure 10. CPF plots for the highest 25 % of the mass contributions at Wilmington site.

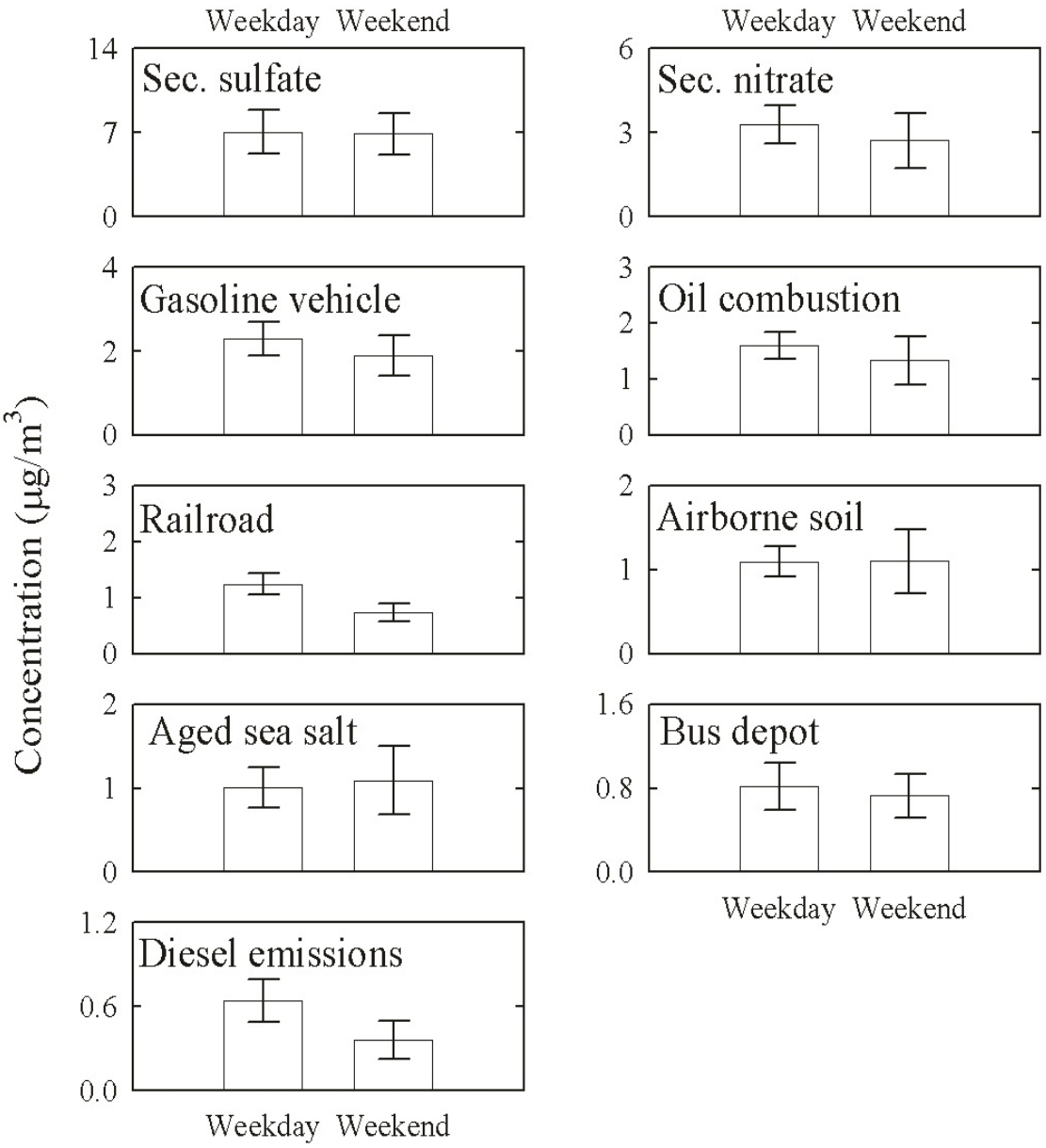

Figure 11. Weekend/weekend variations at Wilmington site.

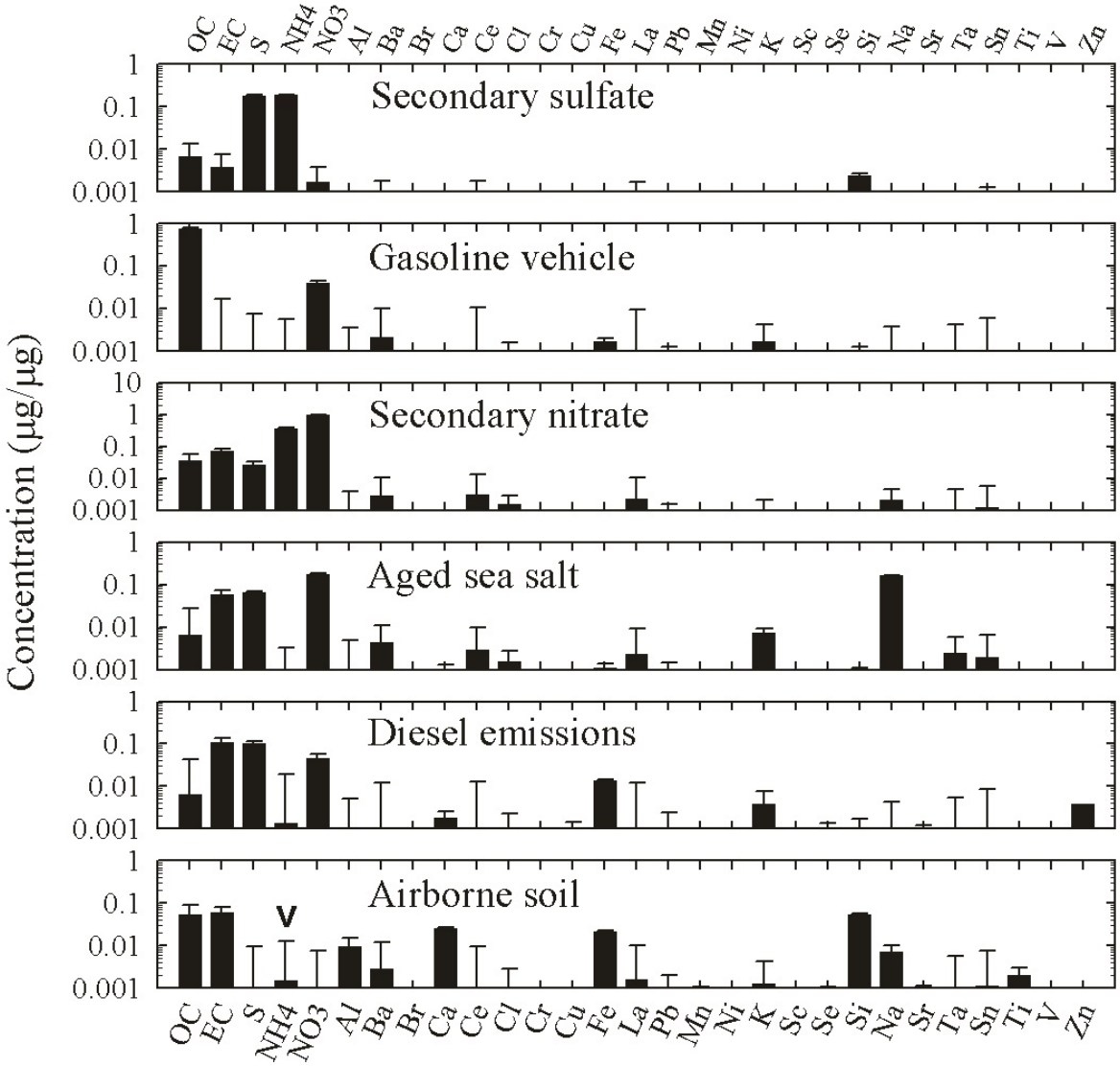

Figure 12. Source profiles deduced from $PM_{2.5}$ samples measured at Dover site (prediction ± standard deviation). The species that was pulled down by FKEY matrix is indicated by arrowhead.

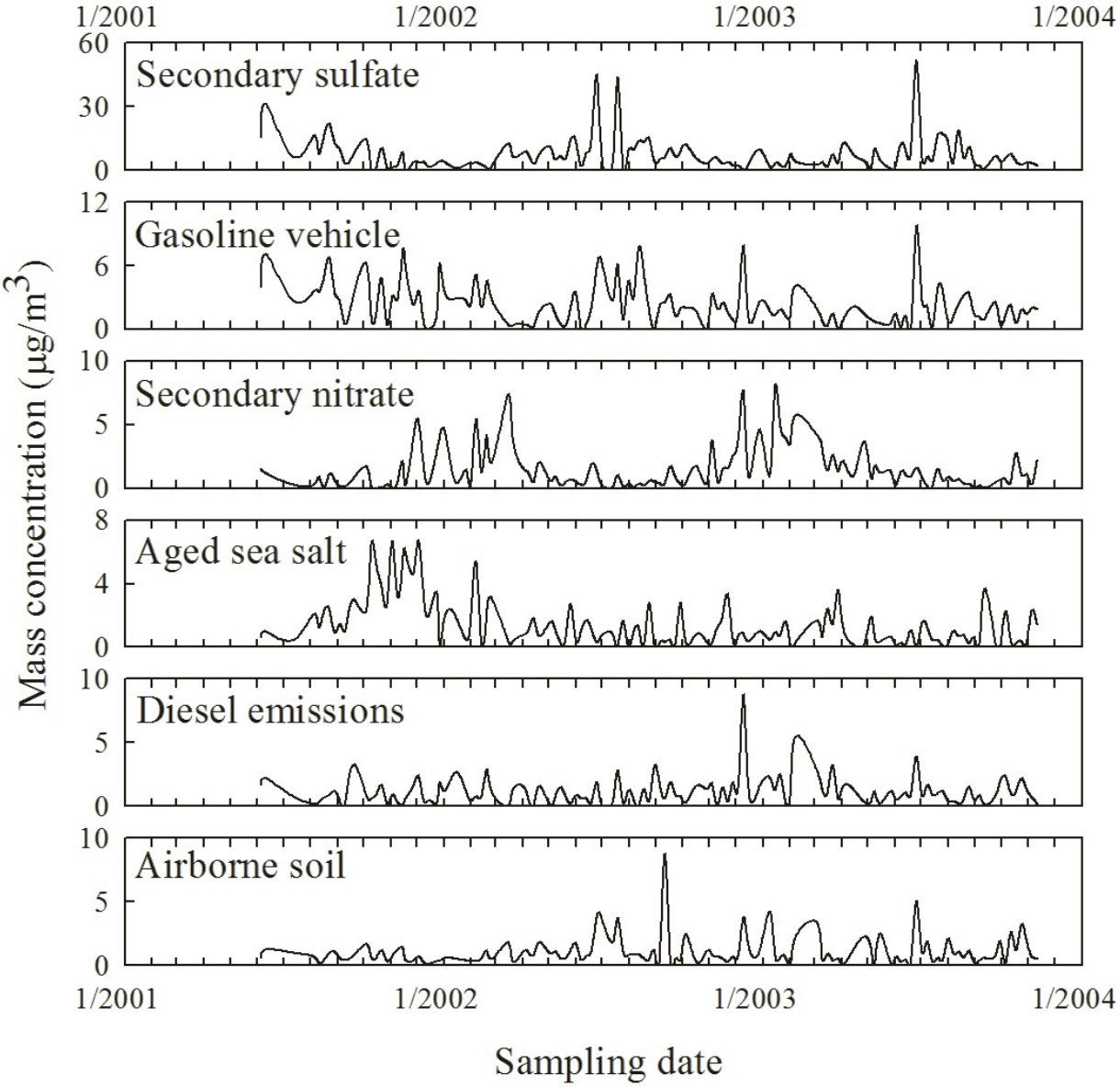

Figure 13. Time series plots of source contributions at Dover site.

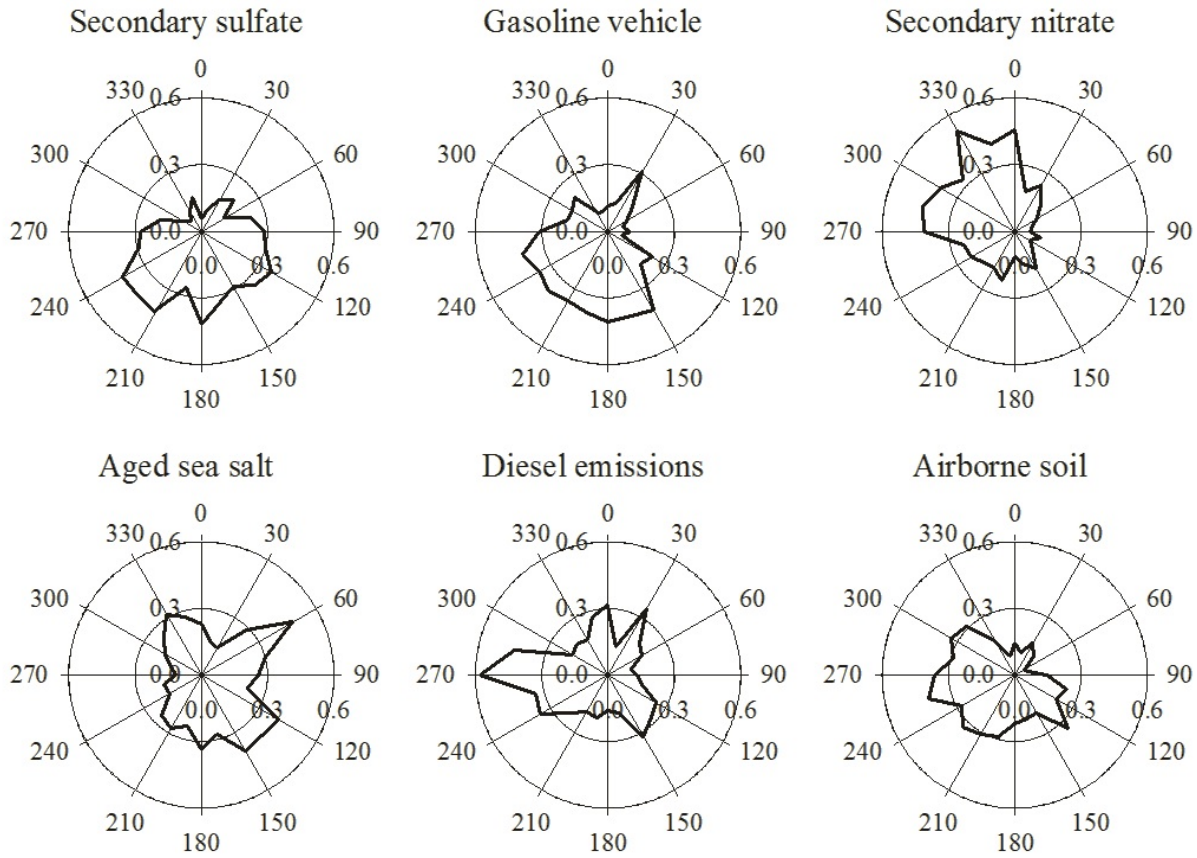

Figure 14. CPF plots for the highest 25 % of the mass contributions at Dover site.

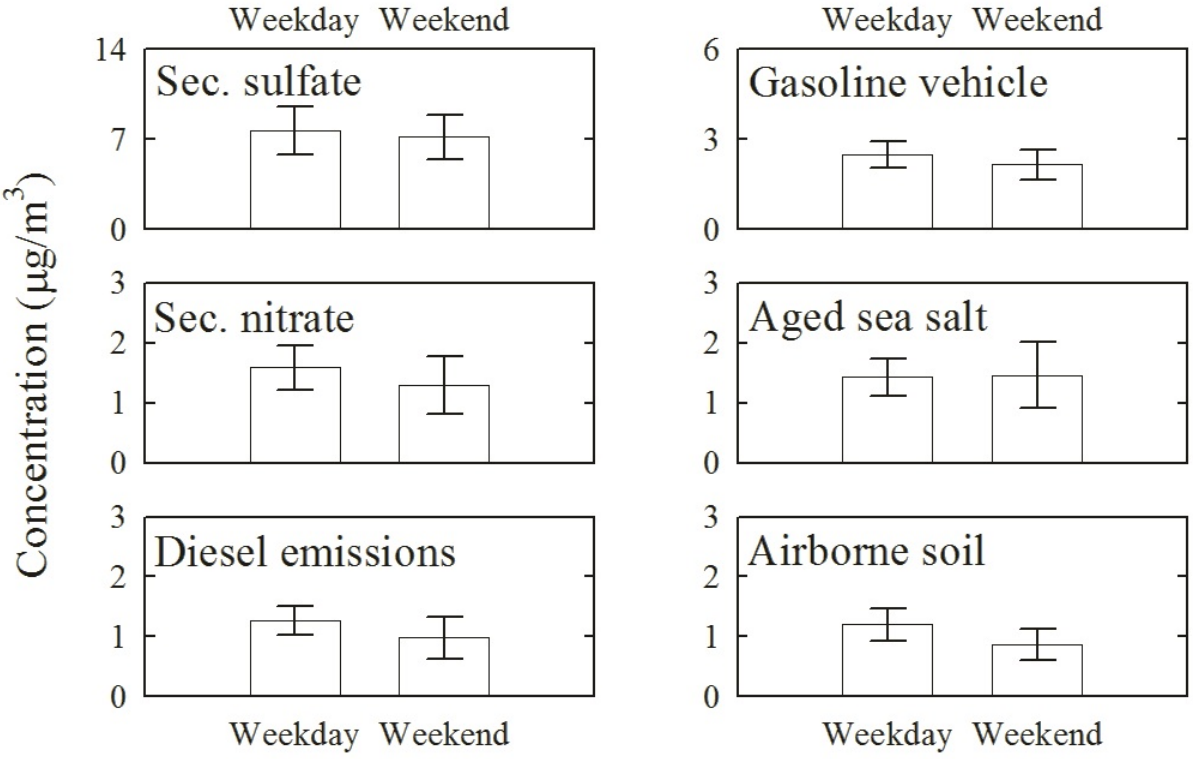

Figure 15. Weekday/weekend variations at Dover site.

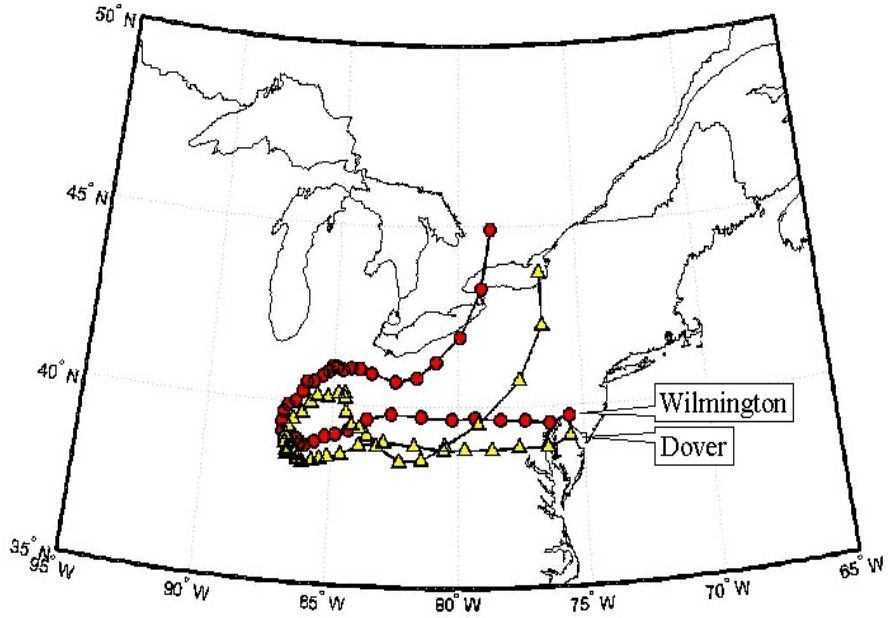

Figure 16. Backward trajectories arriving on July 19, 2002 calculated from NOAA Air Resource Laboratory.

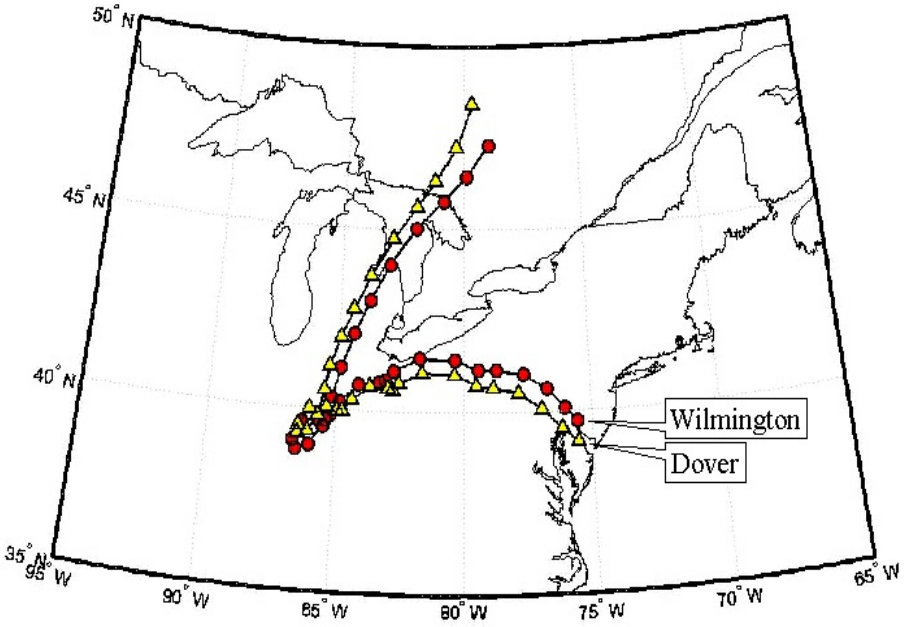

Figure 17. Backward trajectories arriving on June 26, 2003 calculated from NOAA Air Resource Laboratory.

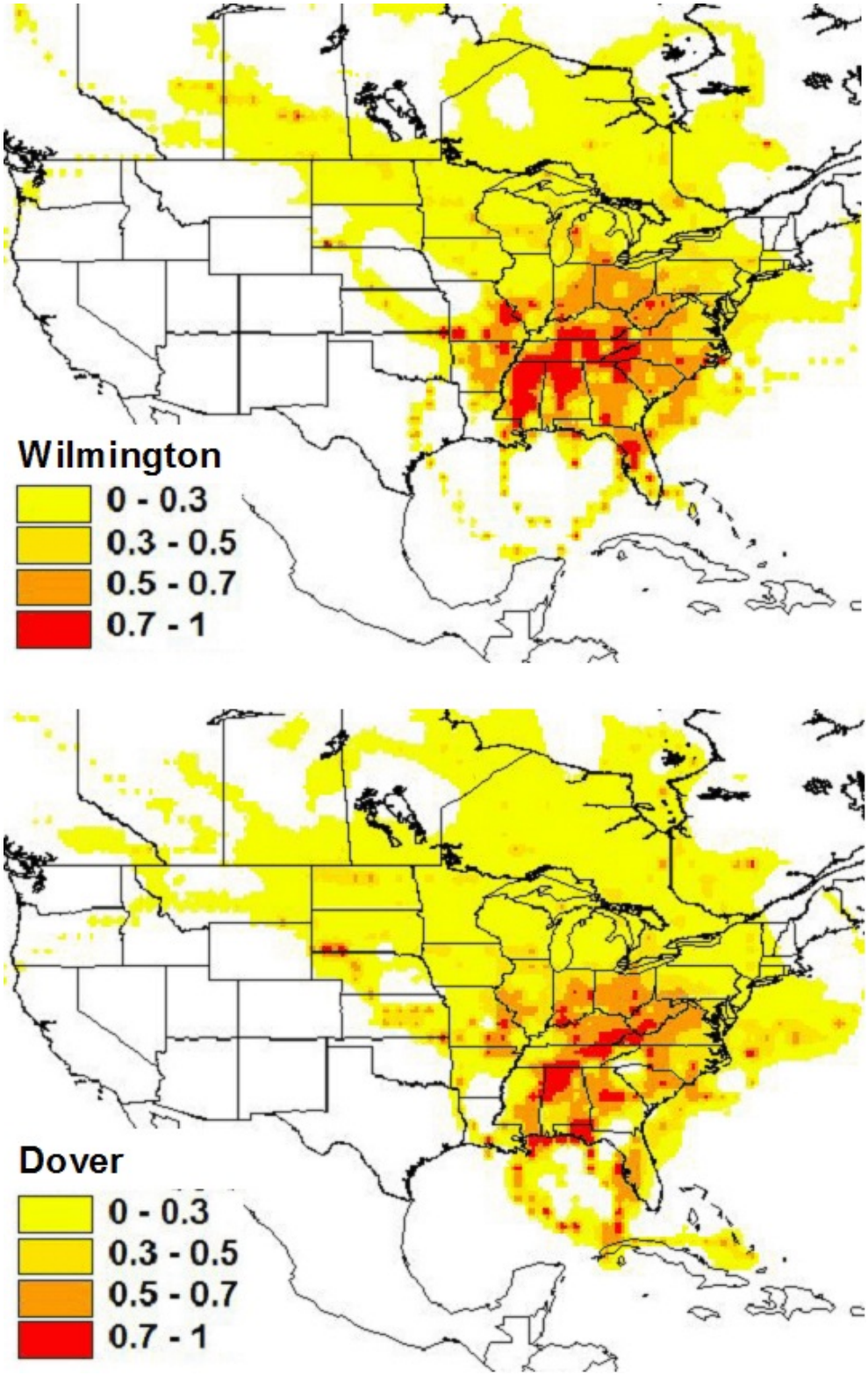

Figure 18. PSCF plots for the secondary sulfate aerosol sources.

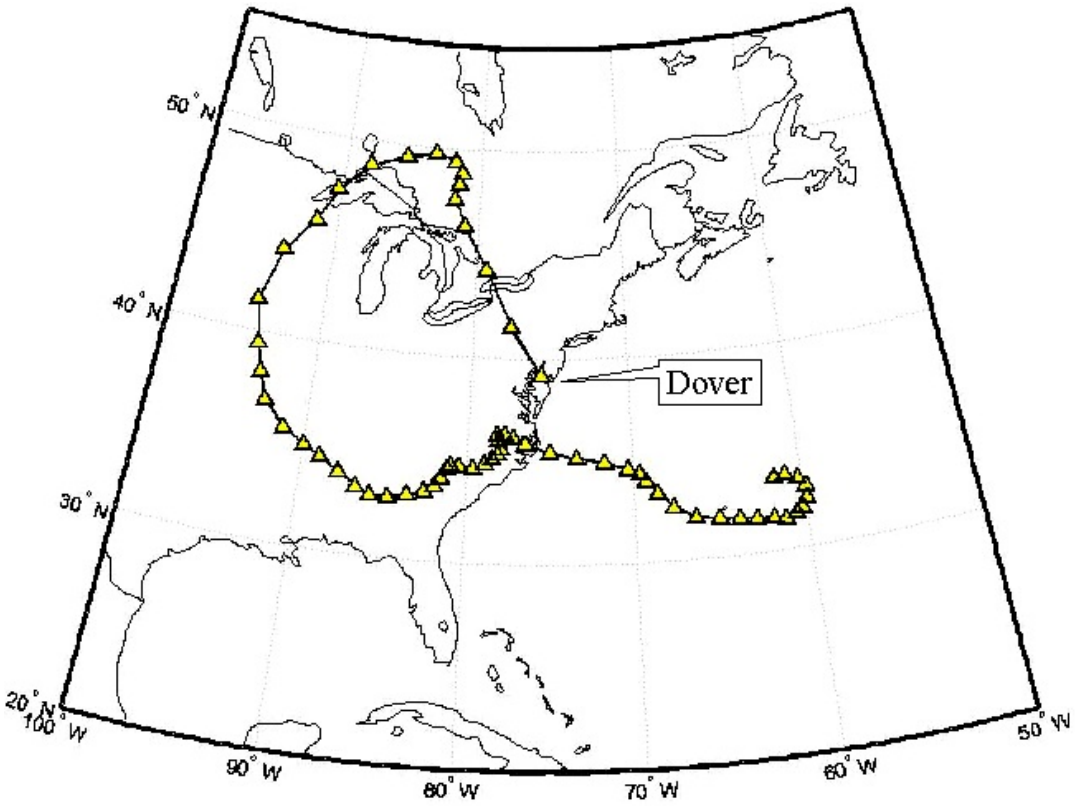

Figure 19. Backward trajectories arriving at Dover, DE on September 11, 2002 calculated from NOAA Air Resource Laboratory.

REFERENCES

Ashbaugh, L.L., Malm, W.C., Sadeh, W.Z. A residence time probability analysis of sulfur concentrations at Grand Canyon National Park, Atmospheric Environment, 19(8), 1263-1270, 1985.

Birch, M.E., Cary, R.A. Elemental carbon-based method for monitoring occupational exposures to particulate diesel exhaust; Aerosol Science and Technology 25, 221-241, 1996.

Bukowiecki, N., Hegedus, F., Falkenberg, G., Gehrig, R., Hill, M., Weingartner, E., Baltensperger, U., Highly time resolved elemental ambient concentrations of railway generated aerosols. European Aerosol Conference, Budapest, Hungary, 2004.

Chueinta, W., Hopke, P.K., Paatero, P. Investigation of sources of atmospheric aerosol at urban and suburban residential area in Thailand by positive matrix factorization. Atmospheric Environment 34, 3319-3329, 2000.

Draxler, R.R., Rolph, G.D. HYSPLIT (HYbrid Single-Particle Lagrangian Integrated Trajectory) Model access via NOAA ARL READY Website (http://www.arl.noaa.gov/ready/hysplit4.html). NOAA Air Resources Laboratory, Silver Spring, MD, 2003.

Gundel, L.A., Lee, V.C., Mahanama, K.R.R., Stevens, R.K., Rau, J.A. Direct determination of the phase distributions of semi-volatile polycyclic aromatic hydrocarbons using annular denuders, Atmospheric Environment, 29, 1719-1733, 1995.

Henry, R.C., Current factor analysis models are ill-posed, Atmospheric Environment, 21, 1815-1820, 1987.

Hering, S., Cass, G. The magnitude of bias in the measurement of $PM_{2.5}$ regression arising from volatilization of particulate nitrate from Teflon Filters, Journal of Air and Waste Management Association, 49, 725-733, 1999.

Hopke, P.K., Receptor modeling in environmental chemistry. John Wiley & Sons, New York, 1985.

Hopke, P.K., Barrie, L.A., Li, S.M., Cheng, M.D., Li, C., Xie, Y.L. Possible sources and preferred pathways for biogenic and non-sea salt sulfur for the high arctic, Journal of Geophysical Research, 100(D8), 16595-16603, 1995.

Kim, E., Larson, T.V., Hopke, P.K., Slaughter, C., Sheppard, L.E., Claiborne, C. Source

identification of $PM_{2.5}$ in an arid northwest U.S. city by Positive Matrix Factorization, Atmospheric Research. 66, 291-305. 2003a.

Kim, E., Hopke, P.K., Edgerton, E. Source identification of Atlanta aerosol by Positive Matrix Factorization, Journal of Air and Waste Management Association. 53, 731-739. 2003b.

Kim, E., Hopke, P.K., Larson, T.V., Naydene, N., Lewtas, J. Factor analysis of Seattle fine particles, Aerosol Science and Technology. 38, 724-738, 2004a.

Kim, E., Hopke, P.K., Edgerton, E.S. Improving source identification of Atlanta aerosol using temperature resolved carbon fractions in Positive Matrix Factorization. Atmospheric Environment. 38, 3349-3362, 2004b.

Kim, E., Hopke, P.K. Source apportionment of fine particles at Washington, DC utilizing temperature resolved carbon fractions. Journal of Air and Waste Management Association, 54, 773-785, 2004a.

Kim, E., Hopke, P.K. Improving source identification of fine particles in a rural northeastern U.S. area utilizing temperature resolved carbon fractions. Journal of Geophysical Research, 109, D09204, 2004b.

Kim, E., Hopke, P.K., Qin, Y. Estimation of organic carbon blank values and error structures of the speciation trends network data for source apportionments. Journal of Air and Waste Management Association, 2005a (In submission).

Kim, E., Hopke, P.K., Kenski, D.M., Koerber, M. Sources of fine particles in a rural midwestern U.S. area. Environmental Science and Technology. 2005b (In submission).

Kim, E., Hopke, P.K., Improving source apportionment of fine particles in the eastern U.S. utilizing temperature resolved carbon fractions. Journal of Air and Waste Management Association, 2005c (In submission).

Koutrakis, P., Wolfson, J.M., Slater, J.L., Brauer, M., Spengler, J.D. Evaluation of an annular denuder/filter pack system to collect acidic aerosols and gases, Environmental Science and Technology, 22, 1463-1468, 1988.

Lee, E., Chun, C.K., Paatero, P. Application of Positive Matrix Factorization in source apportionment of particulate pollutants, Atmospheric Environment, 33, 3201-3212, 1999.

Miller, M.S., Friedlander, S.K., Hidy, G.M. A chemical element balance for the Pasadena aerosol,

Journal of Colloid and Interface Science, 39, 165-176, 1972.

Paatero, P., Least square formulation of robust non-negative factor analysis, Chemometrics and Intelligent Laboratory Systems, 37, 23-35, 1997.

Paatero, P., Hopke, P.K., Song, X.H., Ramadan, Z. Understanding and controlling rotations in factor analytic models, Chemometrics and Intelligent Laboratory Systems, 60, 253-264, 2002.

Paatero, P., Hopke, P.K. Discarding or downweighting high-noise variables in factor analytic models, Analytica Chimica Acta, 490, 277-289, 2003.

Pankow, J.F., Mader, B.T. Gas/solid partitioning of semivolatile organic compounds (SOCs) to air filters. 3. An analysis of gas adsorption artifacts in measurements of atmospheric SOCs and organic carbon (OC) when using Teflon membrane filters and quartz fiber Filters, Environmental Science and Technology, 35(17), 3422-3432, 2001.

Polissar, A.V., Hopke, P.K., Paatero, P., Malm, W.C., Sisler, J.F. Atmospheric aerosol over Alaska 2. Elemental composition and sources, Journal of Geophysical Research, 103(D15), 19045-19057, 1998.

Polissar, A.V., Hopke, P.K., Poirot, R.L. Atmospheric aerosol over Vermont: Chemical composition and sources, Environmental Science and Technology, 35, 4604-4621, 2001.

Ramadan, Z., Song, X. H., Hopke, P.K., Identification of sources of Phoenix aerosol by positive matrix factorization, Journal of Air and Waste Management Association 50, 1308-1320, 2000.

Rolph, G.D., Real-time Environmental Applications and Display sYstem (READY) Website (http://www.arl.noaa.gov/ready/hysplit4.html). NOAA Air Resources Laboratory, Silver Spring, MD, 2003.

RTI, Quality Assurance Projects Plan Chemical Speciation of $PM_{2.5}$ Filter Samples, http://www.epa.gov/ttn/amtic/files/ambient/pm25/spec/rtiqap.pdf, Research Triangle Park, NC, 2004a.

RTI, Extended Semi-Annual Data Summary Report for the Chemical Speciation of $PM_{2.5}$ Filter Samples Project, RTI/07565/06DS, Research Triangle Park, NC, 2004b.

Song, X.H., Polissar, A.V., Hopke, P.K., Source of fine particle composition in the northeastern

U.S., Atmospheric Environment, 35, 5277-5286, 2001.

Tolocka, M.P., Solomon, P.A., Mitchell, W., Norris, G.A., Gemmill, D.B., Wiener, R.W., Vanderpool, R.W., Homolya, J.B., Rice, J., East versus west in the US: Chemical characteristics of $PM_{2.5}$ during the winter of 1999. Aerosol Science and Technology 34, 88-96, 2001.

Watson, J.G., Chow, J.C., Lowenthal, D.H., Pritchett, L.C., Frazier, C.A., Differences in the carbon composition of source profiles for diesel and gasoline powered vehicles, Atmospheric Environment, 28(15), 2493-2505, 1994.

Watson, J.G., Chow, J.C., Source characterization of major emission sources in the Imperial and Mexicali Valleys along the US/Mexico border; The Science of the Total Environment, 276, 33-47, 2001a.

Watson, J.G., Chow, J.C., Houck, J.E. $PM_{2.5}$ chemical source profiles for vehicle exhaust, vegetative burning, geological material, and coal burning in northwestern Colorado during 1995, Chemosphere, 43, 1141-1151, 2001b.